CHAPTER IV

RESULTS AND DISCUSSION

4.1 Rotating Disc Photocatalytic Reactor (RDPR)

4.1.1 Rotating Disc Photocatalytic Reactor (RDPR) materials

All components of this reactor were the commercial types which well known:

- The ultraviolet lamp configuration in this reactor type was 380 nm (TLK 40 Watt /05, 380 nm), in the length of 60 cm. It was applicable for 40 watt and 220 voltages from Fillip Company were used as the source of photoactivity energy.

- The aquarium pumps which provide the flow rate of 900 liter/hours (LIFE TECH-AT1600, 1.1 Hmax, AC200/240 Volt, 50 Hz and 51/60 Watt) were used for supported the continuous flow of wastewater in this work.

- The speed controllable motor in the specification of 1/3 hp (horse power) which appropriate for 220 voltages was selected for control the rotation speed of all catalyst discs plate in RDPR. (ORIENTAL MOTOR-2GN, 7.5K, Max output 6 Watt, 220 Volt, 50/60 Hz and 90-1400/90-1600 RPM)

- The brass valves which corrosive durable were selected for control the flow rate of wastewater.

- Reactor roof was designed in the arc shape which can maximize centralized light energy.

4.1.2 Rotating Disc Photocatalytic Reactor (RDPR) design.

For RDPR, aluminum was appropriate for produced the body of this reactor as it provides high reflection of light to the system. The designed of Rotating Disc Photocatalytic Reactor (RDPR) as shown bellow in Figure 4.1, Figure 4.2 and Figure 4.3 represent the schematic of RDPR for chromium (VI) removal.

The lab scale RDPR consists of 3 major parts including: the wastewater containment, the rotating disc plate which made from stainless steel that had TiO_2 deposited on its surface and the light energy source as ultraviolet lamps.

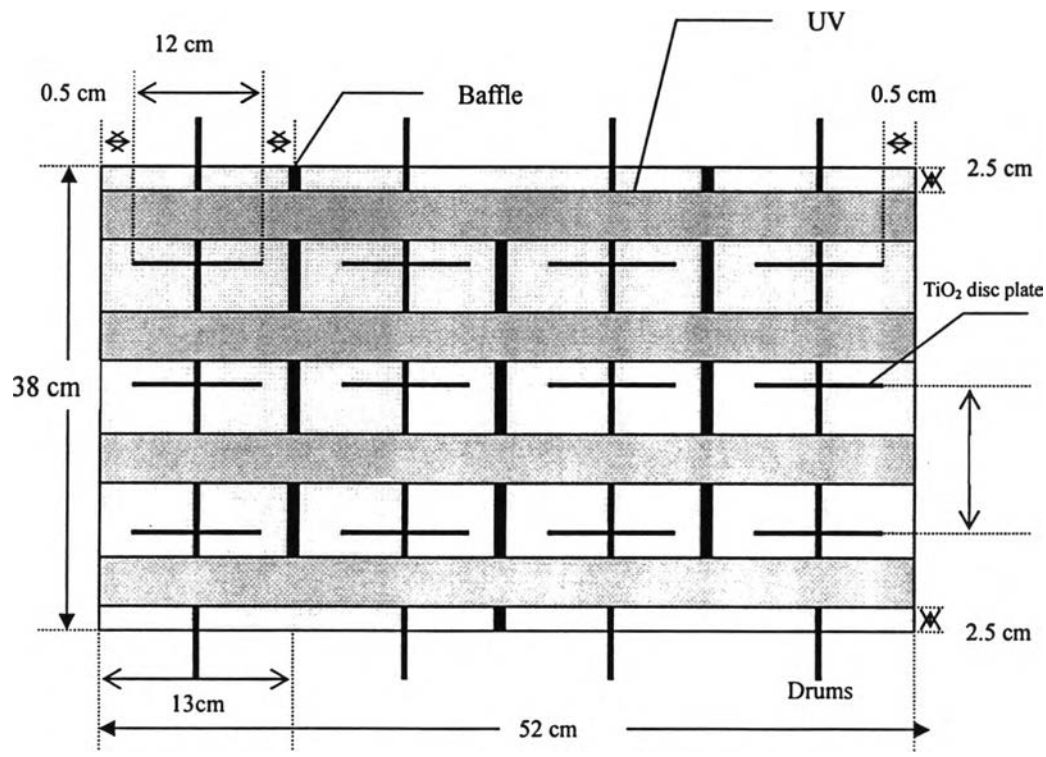

(a)

I 25201633

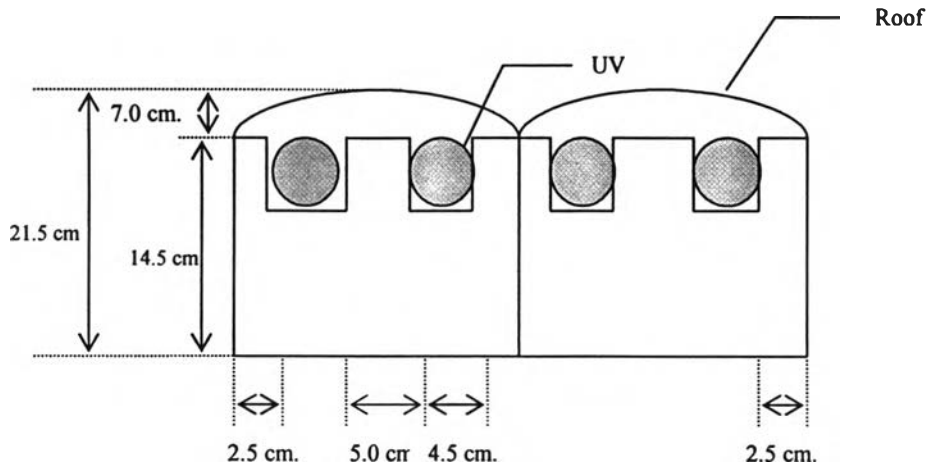
Roof
UV
7.0 cm.
21.5 cm
14.5 cm
2.5 cm.
5.0 cm
4.5 cm.
2.5 cm.

(b)

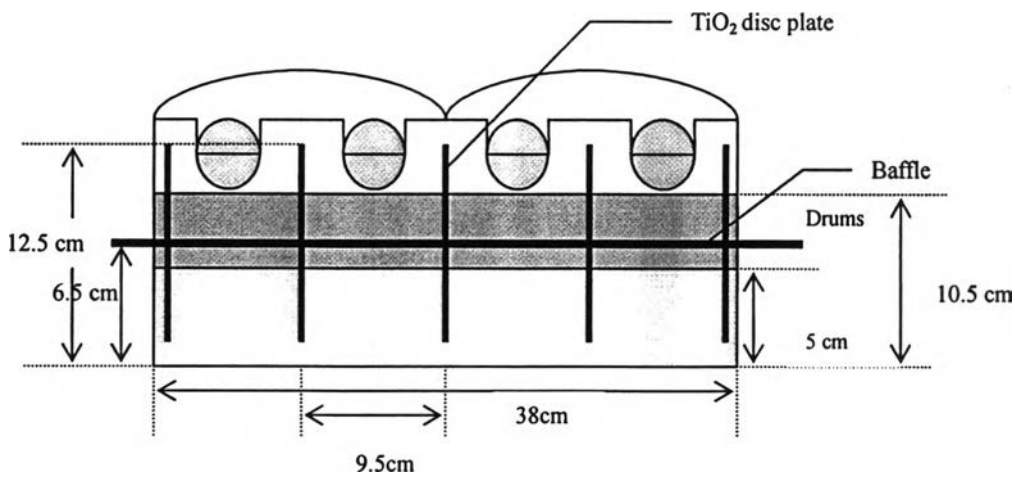
TiO2 disc plate
Baffle
Drums
12.5 cm
6.5 cm
10.5 cm
5 cm
38cm
9.5cm

(c)

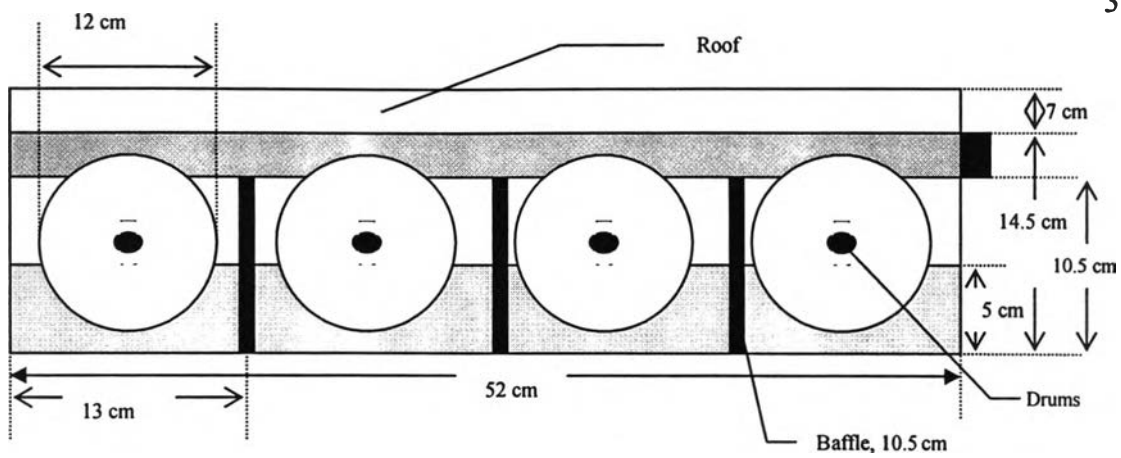

(d)

Figure 4.1 The schematic of RDPR:

(a) The top view of RDPR (b) The front view of RDPR

(c) The front view inside RDPR (d) The side views of RDPR

Table 4.1 Summary of the dimensions of the RDPR shown in Figure 4.1

Function	amount
Length of reactor (cm)	52
Width of reactor (cm)	38
Number of discs	20
Diameters of discs (cm)	12
Thickness of discs (cm)	0.1
Submerge fraction of discs (cm)	4.5
Active surface side (m^2)	0.234
Distance between discs (cm)	9.5

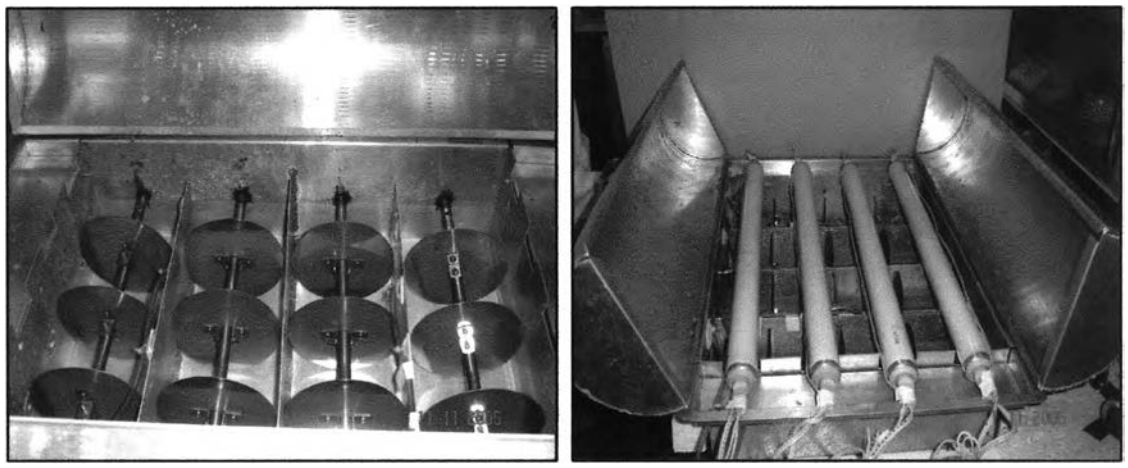

Figure 4.2 The lab scale of Rotating Disc Photocatalytic Reactor (RDPR)

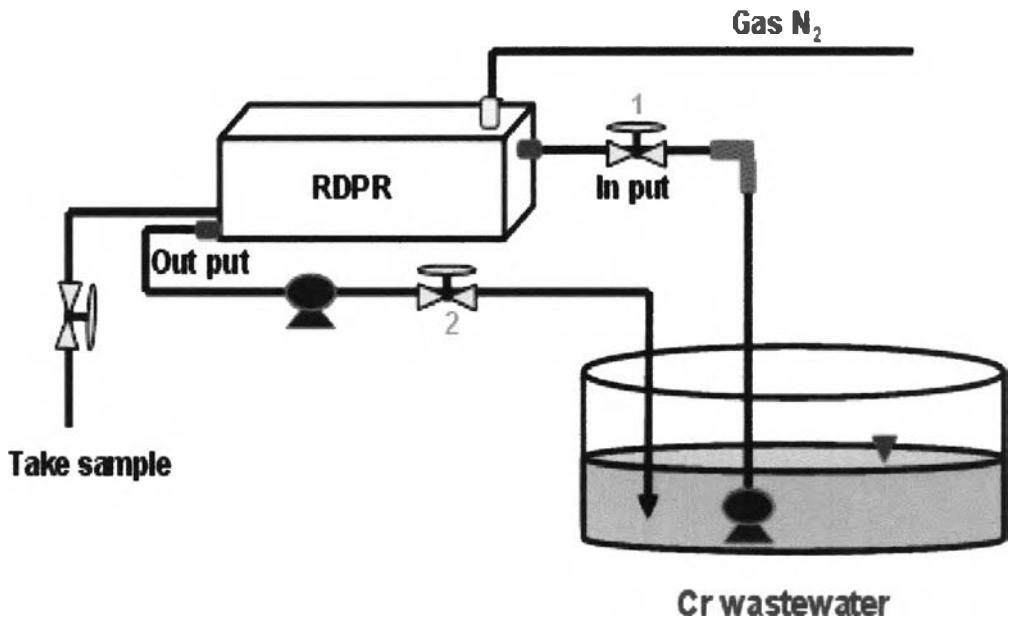

Figure 4.3 The system of chromium (VI) wastewater treatment with RDPR

4.2 The mechanism of chromium (VI) removal by lab scale RDPR.

The mechanism of chromium (VI) removal by lab scale RDPR was explained beneath the photoreduction reaction. This process related to the reduction potential of the pollutant and the catalyst. In this work, the study pollutant was chromium (VI) and the catalyst was TiO_2. The reduction potential of chromium (VI) and TiO_2 present in Figure 2.5.

The mechanism of chromium (VI) removal was started when the thin film TiO_2 disc rotate. The chromium (VI) wastewater carried on the disc plate and the ultraviolet lamp provided the energy to TiO_2 which deposited on the disc plate to let the photocatalysis reaction occur. Then, chromium (VI) in the wastewater reacted with thin film TiO_2. When TiO_2 received the energy more than the band gap (3.2 eV), the electron from valence band (VB) jumped to conduction band (CB). In this study, the study wastewater contains chromium (VI) was receive electron from CB of TiO_2. Then, the chromium changes oxidation state from hexavalence to trivalence which was less toxic species. After reaction, the removal of chromium (VI) from the solution was done by removed the disc plates.

4.3 Thin film characteristic

4.3.1 Thin film characteristic morphology analysis by scanning electron microscope (SEM)

The surface morphology of thin film TiO_2 was analyzed by SEM as shown in Figure 4.4 and 4.5. Figure 4.4 shows the original macroscopic morphology of original stainless steel without any deposition of TiO_2 on the surface. After coated with 3 cycles of TiO_2 thin film which prepared in the ratio of titanium (IV) butoxide: ethanol: HCl: acetylacetone of 1: 30: 0.5: 1 and calcite at 500°C for 30 minutes (Figure 4.5), the boundary was shallow as TiO_2 film covered on stainless grain and surface. This thin film exhibits smooth surface without any crack.

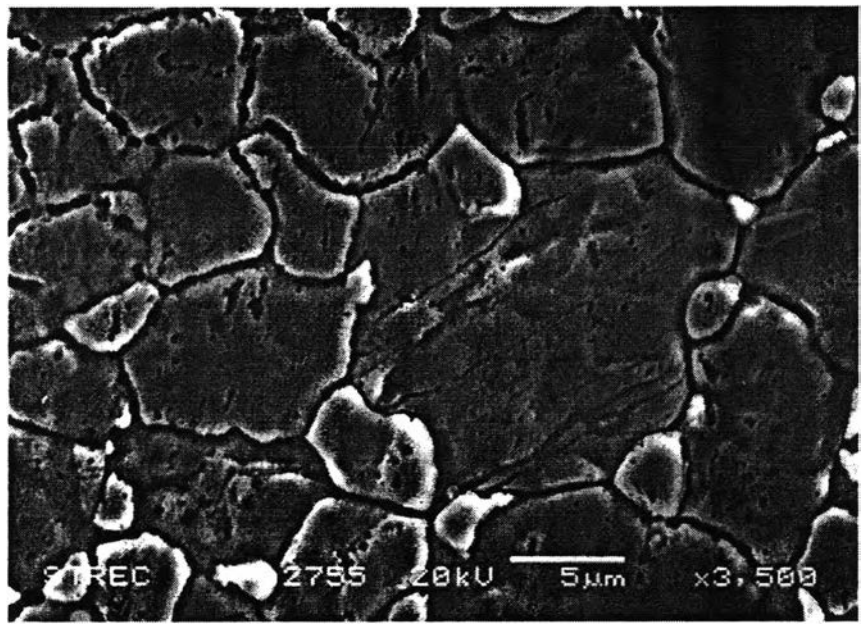

Figure 4.4 stainless steel surfaces without TiO_2 thin film at 3500 × magnifications.

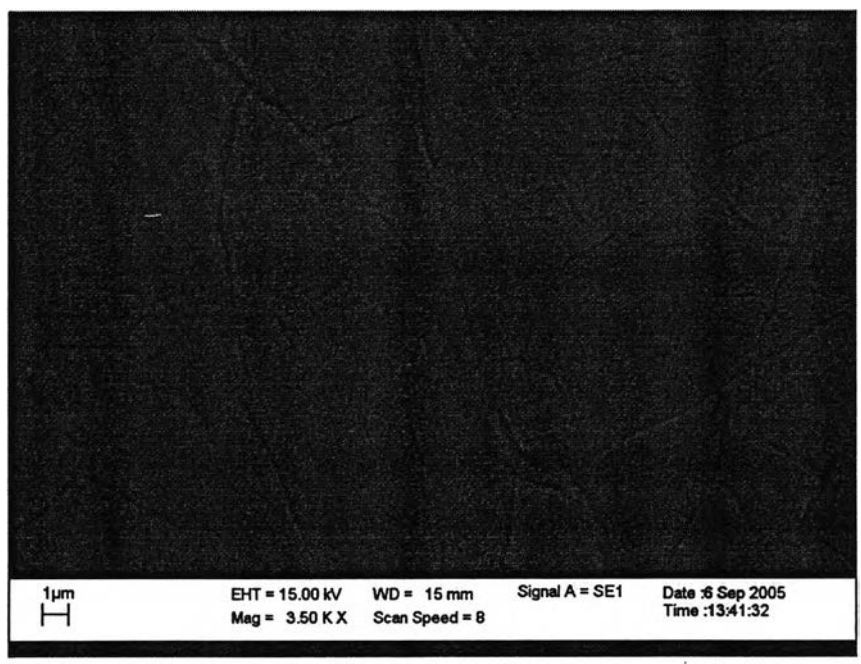

Figure 4.5 SEM of the TiO_2 thin film surface prepared with 3 cycles coated and calcite at 500°C for 30 minutes with 3500 × magnifications.

4.3.2 Thin film characteristic morphology analysis by X-Ray Diffraction (XRD)

The TiO_2 thin films in this work were prepared by the following: 3 coating cycles and calcined at 500 °C calcinations temperature. The X-ray Diffraction (XRD) pattern of thin films in this work is shown in Figure 4.6. With the high amount of anatase showing here, it is expected that this thin film TiO_2 can provide high achievement in chromium (VI) removal.

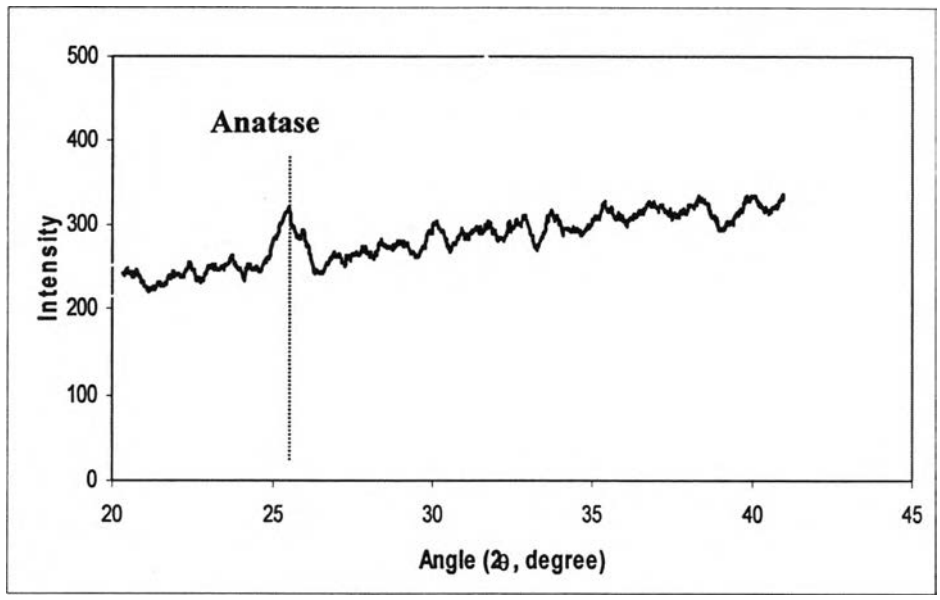

Figure 4.6 The X-ray diffraction (XRD) pattern of thin film TiO_2 which 3 cycle coating at 500°C calcinations temperature for 30 minutes

Figure 4.6 shows the XRD pattern of the TiO_2 thin films which are coated for 3 cycles at 500°C calcinations temperature for 30 minutes. The peak of TiO_2 crystalline was appears as anatase phase with 2θ equal to 25.4 degree. This XRD pattern was used for the crystallite size calculation by line broadening measurements in this equation (Debye-Scherrer):

$$L = \frac{K\lambda}{\beta\cos\theta} \qquad (4.1)$$

where,

L = the crystallite size (nm)

K = the Debye-Scherrer constant (ususlly taken as 0.89)

λ = the wavelength of the X-ray radiation (Cu Kα = 0.15418 nm)

β = the line width at half-maximum height of the broadened peak

θ = the half diffraction angle of the centroid of the peak (degree)

From Figure 4.6, crystallite size of TiO_2 prepared with 3 coating cycles can be calculated as follows:

$$L = \frac{0.89 \times 0.15418}{0.01396 * \cos(25.4/2)} = 10.076 \text{ nm}$$

Thickness of TiO_2 thin film 91 nm which analyst by scanning electron microscope (SEM) as present in Figure 4.7.

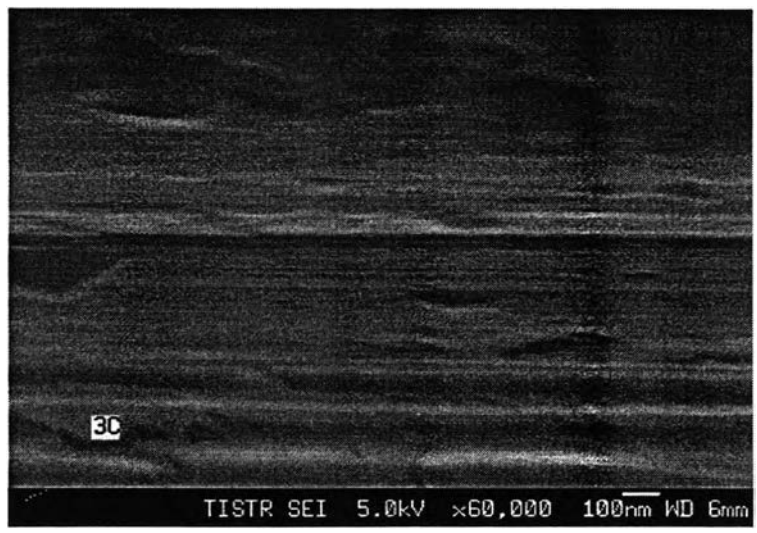

Figure 4.7 Morphology of thin film TiO_2 obtained from SEM showing the thickness of thin film TiO_2 in this work.

Mass of TiO_2 per disc plate was obtained by weighing measurement which is approximate 0.226 mg/cm^2. As one disc plate has area measured by geometric method as 97.48 cm^2, Thus the TiO_2 deposited on the stainless steel disc plate should be equal to 22.03 mg.

4.4 Effect of initial pH of wastewater in the operating of RDPR.

In this experiment part, the effect of initial pH of wastewater was investigated by varying the pH value in the range of acid (pH 3), neutral (pH 7) and basic (pH 11). The initial pH of synthesis wastewater was about 7, thus, in the neutral system it was no need to adjust the initial pH. The adjustment of pH 3 was performed by adding of sulfuric acid (H_2SO_4) and to adjust the initial pH to 11; the chemical used was sodium hydroxide (NaOH) which was the strong basic. The experimental condition for each pH was shown in Table 4.2.

Table 4.2 Experimental details in the study of the effect of initial pH of wastewater on chromium (VI) removal efficiency.

Function	amount
Concentration of wastewater, ppm	25
Chromium (VI) loading in one experiment (25 mg/L * 20 L), mg	500
Wastewater flow rate (Q_w), mL/sec	90
Rotating disc speed (V_r), rpm	200
TiO_2 coating surface area, m^2	0.234
Height of wastewater in RDPR, cm	5
Rate of N_2 Gas input, L/min	4.5

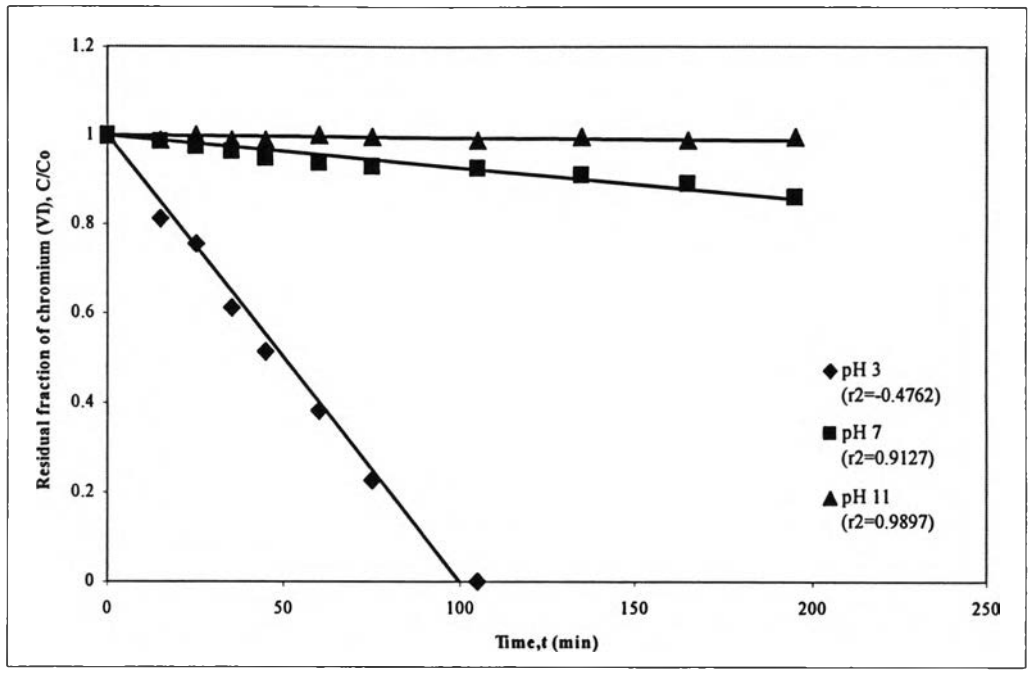

Figure 4.8 Residual fraction of chromium (VI) in different pH of wastewater

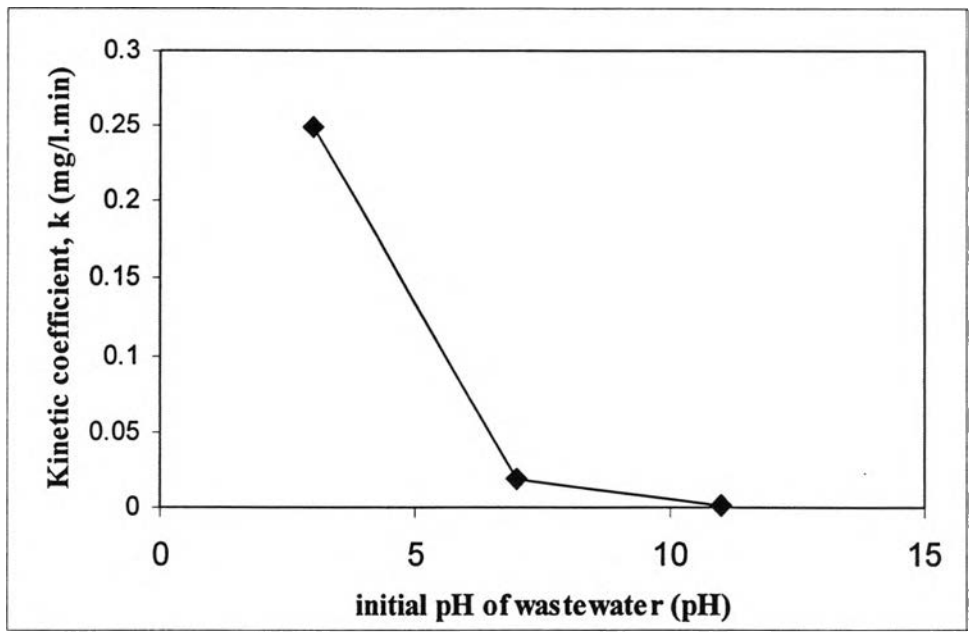

Figure 4.9 Kinetic coefficients (k) of residual chromium (VI) with different pH of wastewater.

Table 4.3 Experimental conditions of each experiment in varying initial pH of wastewater.

Experimental condition	Experiment No.		
	1	2	3
Initial pH of wastewater	3	7	11
Cr (VI) removal percentage If reaction period is 105 min, %	100	0.715	0.0525
Kinetic coefficient (k), mg/L.min	0.2492	0.0183	0.0009

Figure 4.8 presents the effect of initial pH of wastewater on photoreduction of chromium (VI). The result was shown that when the initial pH of wastewater was basic (pH 11) the reaction cannot remove chromium (VI) at all. In natural pH (pH 7), the photocatalysis reaction can be occurred but the reaction rate was relatively low. Then, the removal of chromium (VI) need longer time to complete. In contrast pH 3 provided the highest efficiency removal of chromium (VI) which required the reaction time to complete in chromium (VI) removal as 105 minutes with 0.2492 mg/L.min of kinetic coefficient as shown above.

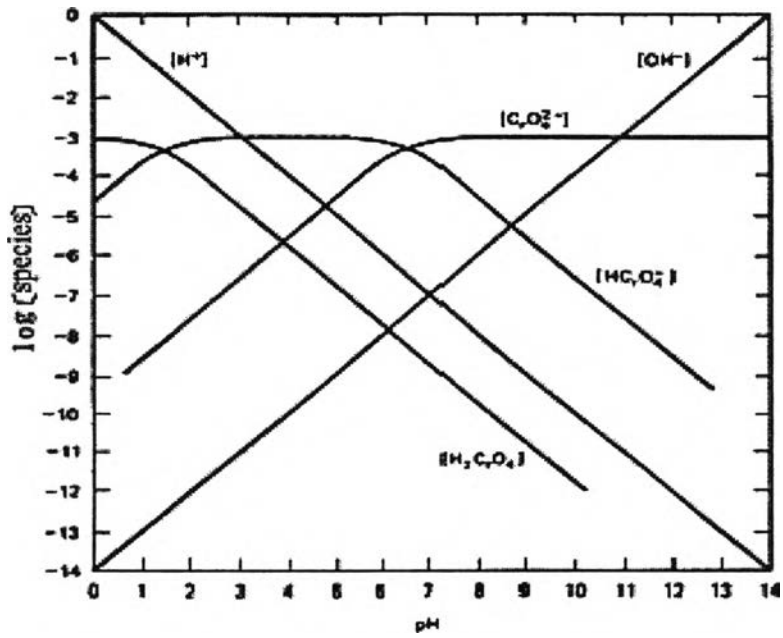

Figure 4.10 Show the compound of chromium (VI) in the solution which different pH (Ku et. al., 2001)

In general, the chromium (VI) can form many complex compounds as CrO_4^{2-} and $HCrO_4^-$ depend on the concentration of chromium (VI) and pH value of the solution. The information from Figure 4.10 found that at strong acidic condition, pH 0 - 1.8, the predominant species of chromium (VI) was H_2CrO_4. In the pH range of 1.8 – 7, chromium (VI) was in the form of $HCrO_4^-$ and at basic pH, pH more than 7, chromium (VI) was in the form of CrO_4^{2-}. Accordingly, initial pH of wastewater is directly affected to the efficiency of chromium removal.

Result from this experimental could be supported by the study of Lin et al. (1993) who presented the changing in the potential value of valence band (VB) and conduction band (CB) of TiO_2 was changed following the pH of the solution. It could be explained that when increasing pH of the solution, it was reduced the potential value of the band gab of TiO_2 as call *Nerstain* as change -59 mv in every changing pH at 25 °C (-59 mv/ pH Unit at 25 °C). Therefore, pH of the solution affects to the efficiency in chromium (VI) removal by the difference between the reduction potential of chromium (VI) in each forms and conduction band (CB) of TiO_2.

In basic pH, the different values between the reduction potential of CrO_4^{2-} and conduction band (CB) of TiO_2 was smaller than acidic pH as shown in Figure 2.2. In the same way, the different values between the reduction potential of $HCrO_4^-$ and conduction band (CB) of TiO_2 in acidic pH is high. Then the photoreduction of chromium (VI) provide high efficiency in acidic pH. Thus, Cr^{6+} was changed to Cr^{3+} which less toxic species at acidic pH as shown in the experiment.

4.5 Effect of wastewater flow rate (Q_w) in the operating of RDPR

Flow rate of wastewater is an important parameter in the operating of continuous mode reactor. The values of flow rate are relative to treating cycle of wastewater which is direct proportion to the efficiency of chromium (VI) removal. In this experiment set, flow rates of wastewater were experimented with other fixed parameters presented in Table 4.4. The varying wastewater flow rates consisted of 20,

40, 60, 80 and 90 mL/sec. The results of this experiment set investigated by the analysis of residual chromium (VI) concentration in wastewater.

The residual fraction of chromium (VI) was calculated as follow:

$$\text{Residual fraction} = \frac{C_t}{C_o} \qquad (4.2)$$

Where,

C_t is the concentration of chromium (VI) in wastewater at time, ppm

C_o is the initial concentration of chromium (VI) in wastewater, ppm

Table 4.4 Experimental details in the study of the effect of wastewater flow rate (Q_w) on chromium (VI) removal efficiency.

Function	amount
Concentration of wastewater, ppm	25
Chromium (VI) loading in one experiment (25 mg/L * 20 L), mg	500
Rotating disc speed (V_r), rpm	50
Height of wastewater in RDPR, cm	5
TiO_2 coating surface area, m^2	0.234
Initial pH of wastewater	3
Rate of N_2 Gas input, L/min	4.5

Results of the photocatalytic reduction of chromium (VI) using RDPR using the wastewater flow rate as of 20, 40, 60, 80 and 90 mL/secec and the kinetic coefficients (k) of each wastewater flow rate are shown in Figure 4.11 and Figure 4.12 respectively. Table 4.5 shows the experimental conditions used in each wastewater flow rates.

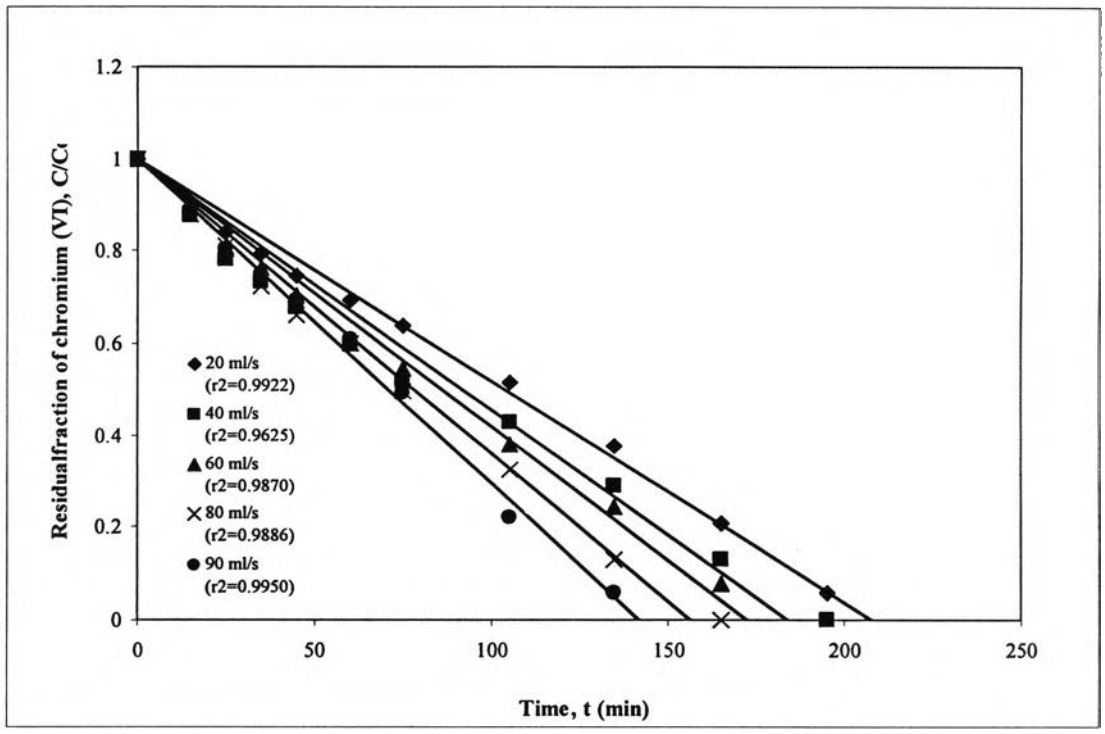

Figure 4.11 Residual fraction of chromium (VI) concentration in different wastewater flow rate.

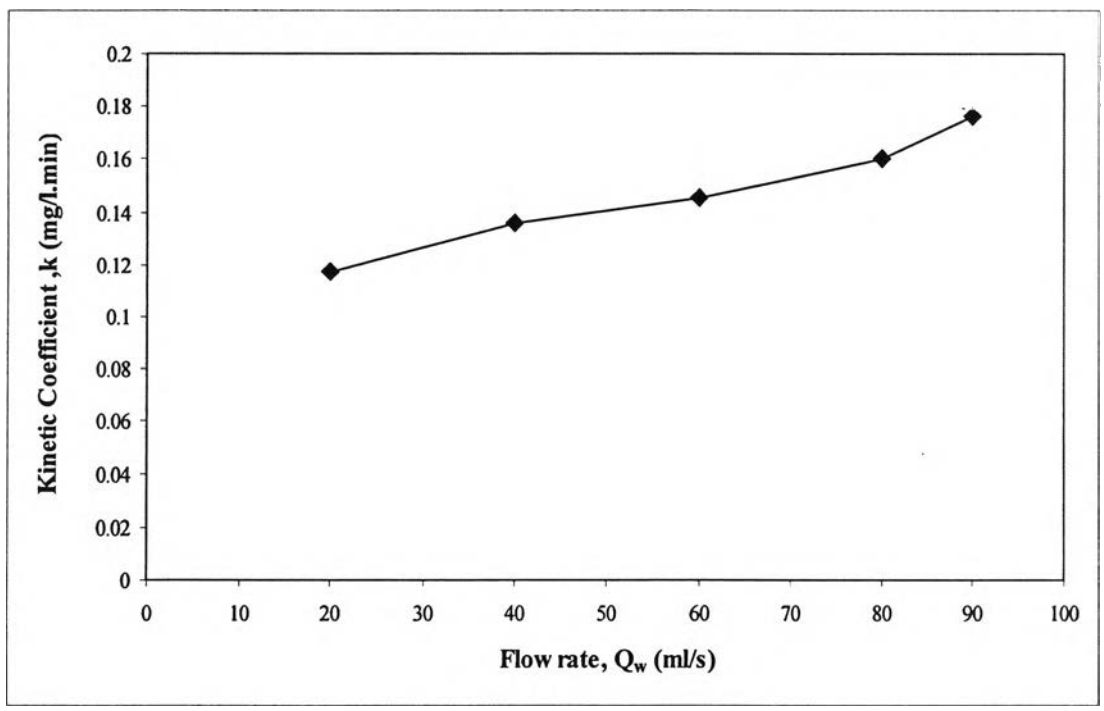

Figure 4.12 Kinetic coefficients (k) of residual chromium (VI) with different wastewater flow rate.

Table 4.5 Experimental conditions of each experiment in varying wastewater flow rates.

Experimental conditions	Experimental No.				
	1	2	3	4	5
Flow rate, mL/sec	20	40	60	80	90
Contact time, min/cycle if reaction period is 143 min	8.41	4.2	2.8	2.1	1.86
Treating cycle, cycle if reaction period is 143 min	17	34	51	68	77
Cr (VI) removal percentage if reaction period is 143 min, %	68.75	77.3	83.14	91.67	100
Kinetic coefficient (k), mg/L.min	0.1174	0.1359	0.1452	0.1601	0.176
Reaction time to complete photoreduction of Cr (VI), min	208	185	172	156	143

Figure 4.11 was shown the relation of residual fraction of chromium (VI) as a function of time. The results can be noted that high efficiency in chromium removal is obtained with the high flow rate of wastewater.

In kinetic consideration, the chromium (VI) removal was representing in zero order pattern which can be represented by the following equation:

$$d[C]/dt = -k[C]^n \qquad (4.3)$$ at zero order, $n = 0$

$$C - C_o = -k.t \qquad (4.4)$$

Figure 4.12 presented that the highest of wastewater flow rate bring highest kinetic coefficient (k) and Table 4.5 presented the experimental condition of each flow rate. From Table 4.5 was found that the specificant parameter that plays a major role in effect of wastewater flow rate in the operating of RDPR was treating cycle. At the highest flow rate 90 mL/secec, the treating cycle were 77 cycles lead to the value of kinetic coefficient as 0.176 mg/L.min. While at the lowest flow rate 20 mL/sec in the same experimental time which had 17 treating cycle, the kinetic coefficient was reduced to 0.1174 mg/L.min.

Information obtained from this graph shown that the increasing of rate constant corresponds to the increasing of flow rate. The values of rate constant were slowly increased with the flow rate of waste stream in the range of 20 – 80 mL/sec. Beyond 80 mL/sec, the rapid increase of chromium removal rate was clearly seen. This behavior may result from the increase of treatment cycle of wastewater. The more cycles for wastewater in one batch, the high amount of chromium could be removed from wastewater. The highest flow rate (90 mL/sec) provided highest efficiency in chromium removal depending on the high number of treatment cycle of wastewater in one batch.

Treatment cycle of wastewater is directly depend on the flow rate of wastewater, as at 90 mL/sec has 77 treating cycles in contrast at 20 mL/sec has 17 treating cycles. Treating cycle is the important point which provides the increasing of chromium (VI) removal. Wastewater velocity is the function of flow pattern which is related to the degree of wastewater mixing, turbulence type, cause to the high mass transfer coefficient. Then, the increase of wastewater flow rate is the increase of chromium (VI) removal efficiency for RDPR reactor.

4.6 Effect of rotating disc speed (V_r) in the operating of RDPR

In this part, flow rate of wastewater 90 mL/sec were fixed as the initial conditions because this flow rate give high efficiency result from previous part, while rotating disc speed were varied from 10 to 50, 100, 150 and 200 rpm respectively as shown in Table 4.6. Results of this experiment set are shown in Figure 4.13.

Table 4.6 Experimental details in the study of the effect of rotating disc speed (V_r) in on chromium (VI) removal efficiency.

Function	amount
Concentration of wastewater, ppm	25
Chromium (VI) loading in one experiment (25 mg/L * 20 L), mg	500
Wastewater flow rate (Q_w), mL/sec	90
Height of wastewater in RDPR, cm	5
TiO_2 coating surface area, m^2	0.234
Initial pH of wastewater	3
Rate of N_2 Gas input, L/min	4.5

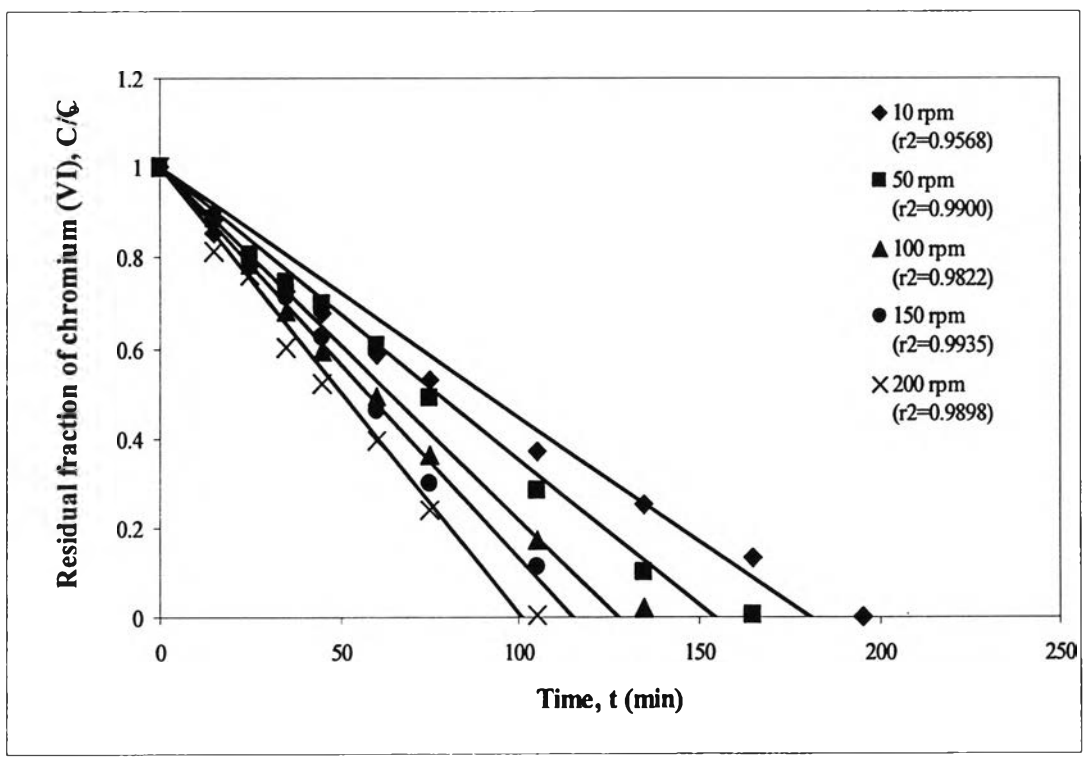

Figure 4.13 Residual fraction of chromium (VI) on time in varies rotating disc speed

It was found that the rotating disc speed promoted the photocatalytic reaction of chromium (VI) removal in the difference results. The faster of rotating disc speed affects on the increasing of chromium (VI) removal rate. With 10 rpm rotating disc speed, the chromium (VI) was completely removed within 182 minutes, while the reaction period was reduced to approximately 100 minutes with 200 rpm rotating disc speed. The fastest rotating disc speed 200 rpm provided the best result of the photoactivity.

As described earlier, the kinetic pattern in chromium (VI) removal using rotating disc photoreactor was performed as zero order; the plotted of kinetic coefficient versus rotating disc speed is shown in Figure 4.14 and the values of kinetic coefficient from each condition were calculated and shown in Table 4.7.

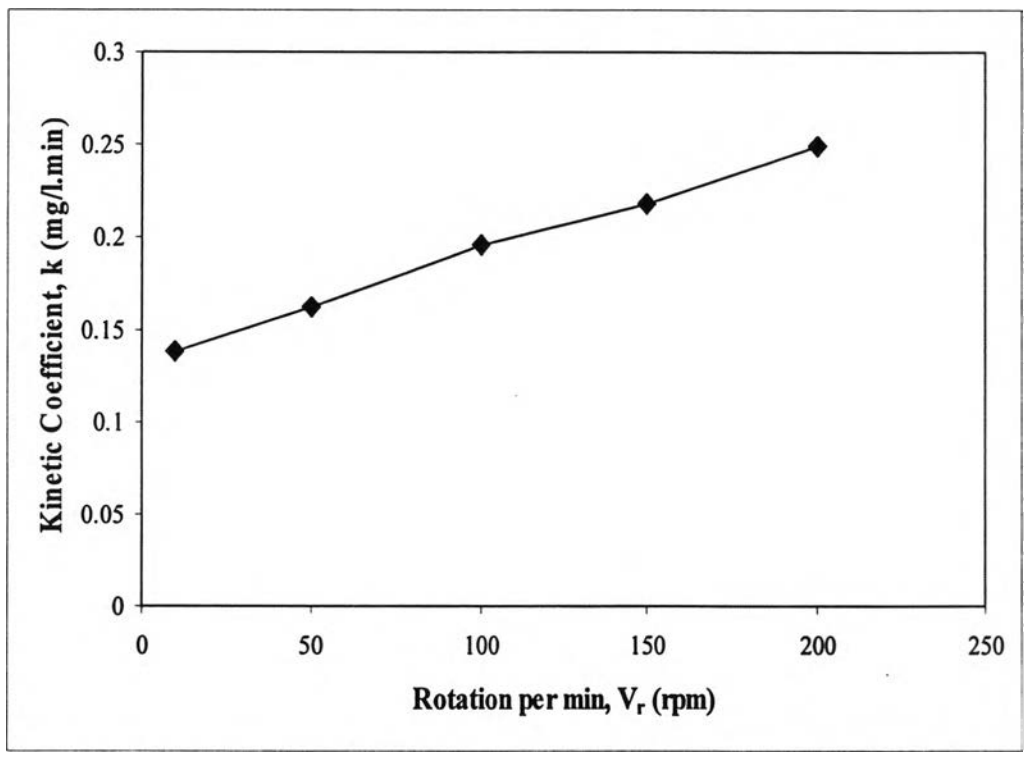

Figure 4.14 Kinetic coefficients (k) of residual chromium (VI) with different rotating disc speed.

Table 4.7 Experimental conditions of each experiment in varying rotating disc speed.

Experimental conditions	Experimental No.				
	1	2	3	4	5
Rotating speed disc, rpm	10	50	100	150	200
Total rotating round in 105 min, round	1050	5250	10500	15750	21000
Contact time for each round, min	0.1	0.02	0.01	0.0067	0.005
TiO_2 coating surface area for 105 min, m^2	245.65	1228.25	2456.5	3684.75	4913
Cr (VI) removal percentage If reaction period is 105 min, %	57.69	68.18	82.03	91.3	100
Kinetic coefficient (k), mg/L.min	0.1384	0.1620	0.1958	0.2173	0.2489
Reaction time to complete photoreduction of Cr (VI), min	182	154	128	115	105

Information obtained from Figure 4.14 and Table 4.7 shown that the values of kinetic coefficient are continuously increased as a function of rotating disc speed, in the range of 10 –200 rpm. The major parameter which plays an important role here was the rotating rounds of TiO_2 disc plate as shown in Table 4.7. The total rotating rounds of disc plate increase from 1050 to 21000 in the rotating speed disc in the range of 10 to 200 rpm. As same the increasing of wastewater flow rate, the increasing of rotating rounds can provide the increasing of wastewater mixing pattern. The completely mix of wastewater (CSTR, continuous stirred tank reactor) is the important parameter that necessary for continuous mode reactor. It is the major parameters which provide the high efficiency of chromium (VI) removal. The more rotating round of TiO_2 disc plate, the high amount of chromium can be removed from wastewater. The highest rotating disc speed at 200 rpm provided the highest value of chromium removal rate constant as equal to 0.2489 mg/L.min. The results from this experiment part suggested that, at high rotating disc speed, the rotating speed of disc was directly effect to the removal efficiency of chromium (VI) in this type reactor.

Finding from this work was well agreement with the research works of Noel et al (2000) and Dionysiou et al (2002). They found that the rate constant increased with increasing of disc angular velocity. The increasing in rotating speed of disc in the range of 10 – 200 rpm could promote the photoreaction rate in this work. Moreover the highly efficiency degradation rate will respond to the intensity of light and the

increasing of contaminant concentration.

4.7 Effect of TiO_2 coating surface area in the operating of RDPR.

TiO_2 coating surface area is the available area on the disc plate that coated with the catalyst or TiO_2 providing the photocatalysis reaction in RDPR as shown in Figure 4.15.

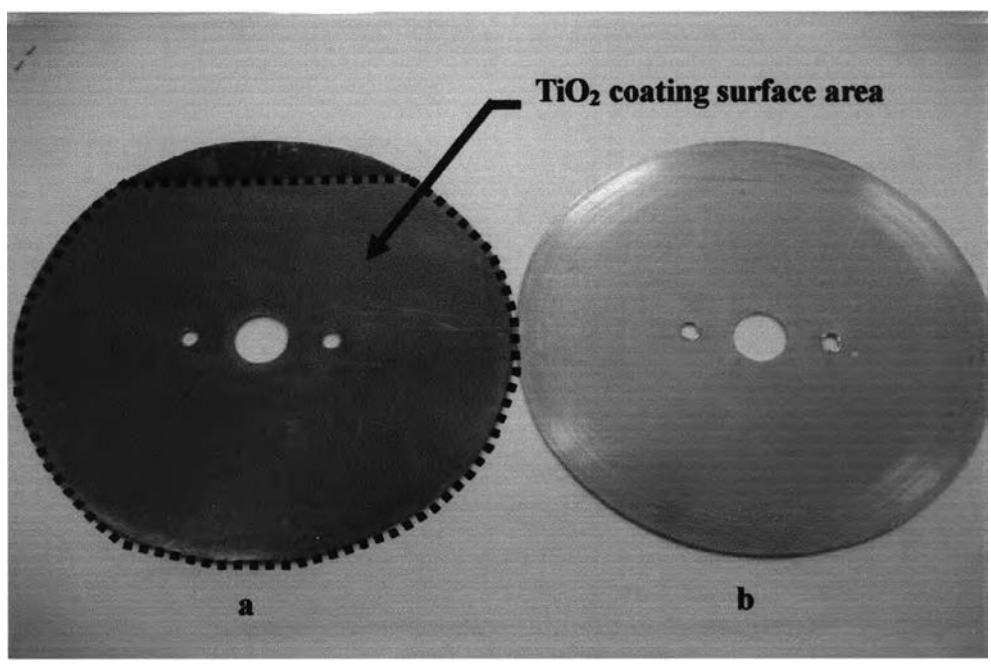

Figure 4.15 Shown the disc plate that use in RDPR.

a. TiO_2 coating surface area of disc plate that coated with TiO_2 in 3 cycles and calcite at 500°C for 30 minutes

b. Disc plate without any TiO_2 thin film

In this experimental part, the fixed parameters used in all experiments were presented in Table 4.8. To study effect of TiO_2 coating surface area on chromium (VI) removal efficiency, the optimum flow rate of wastewater as of 90 mL/sec from the previous section and the optimum rotating disc speed as of 200 rpm were used in this section. TiO_2 coating surface areas of rotating discs plate were varied as 0.117 m^2, 0.1754 m^2, 0.234 m^2, 0.263 m^2 and 0.2924 m^2. Figure 4.16 was shown the results of chromium (VI) removal using RDPR in the different amount of TiO_2 coating surface area. The information of this experimental part which was used in photocatalytic reduction process can be explained in Table 4.9.

Table 4.8 Experimental details in the study of the effect of TiO_2 coating surface area on chromium (VI) removal efficiency.

Concentration of wastewater, ppm	50
Chromium (VI) loading in one experiment (50 mg/L * 20 L), mg	1000
Wastewater flow rate (Q_w), mL/sec	90
Rotating disc speed (V_r), rpm	200
Height of wastewater in RDPR, cm	5
Initial pH of wastewater	3
Rate of N_2 Gas input, L/min	4.5

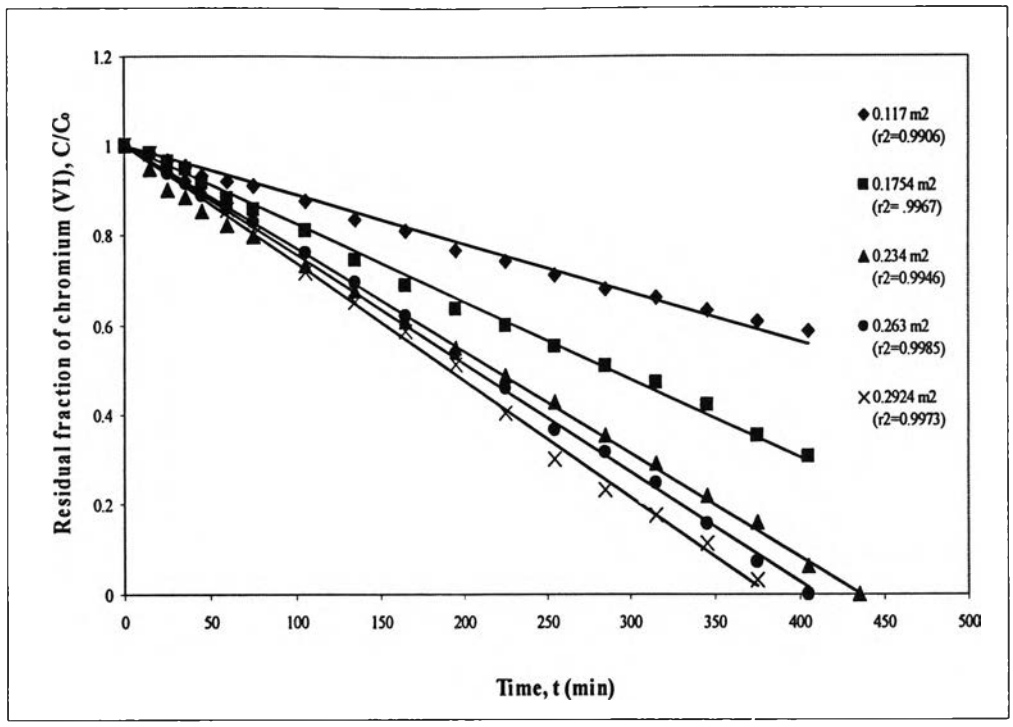

Figure 4.16 Residual fraction of chromium (VI) on time in varies TiO_2 coating surface area

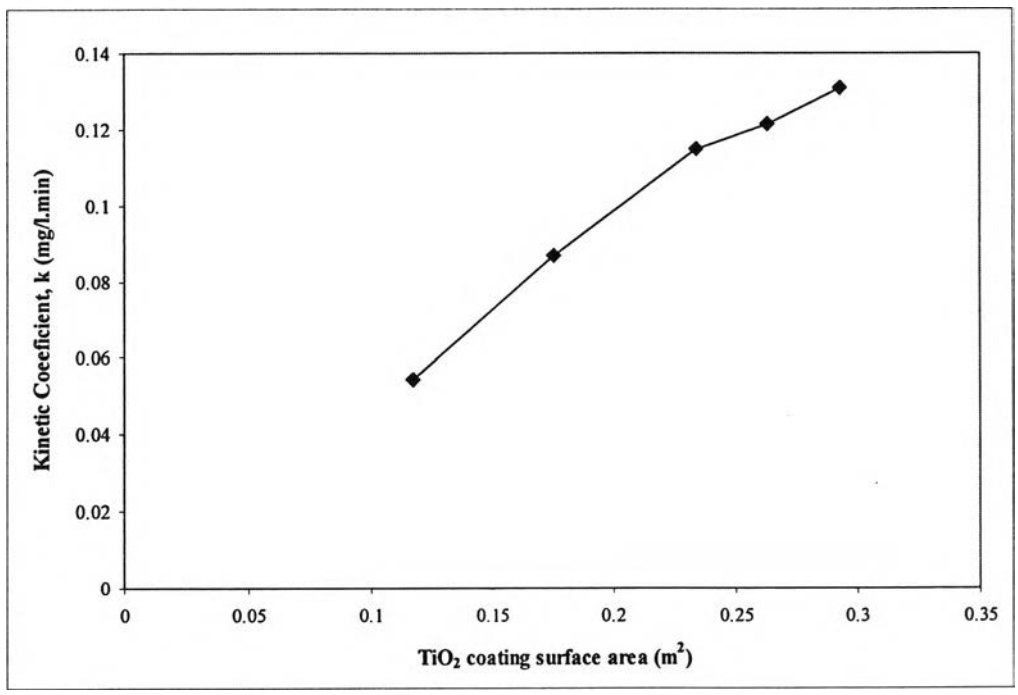

Figure 4.17 Kinetic coefficients (k) of residual chromium (VI) with different TiO_2 coating surface area

The interested experimental condition which can identify the efficiency of the photoreduction reaction is the kinetic coefficient (k). It was found that the kinetic coefficient (k) was a function of TiO_2 coating surface area as represented that increasing of TiO_2 coating surface area was more respond to the increasing of kinetic coefficient (k) values which shown in Figure 4.17.

Table 4.9 Experimental conditions of each experiment in varying TiO_2 coating surface area

Experimental condition	Experimental No.				
	1	2	3	4	5
TiO_2 coating surface area, m^2	0.1170	0.1754	0.234	0.263	0.2924
Amount of TiO_2 used in one experiment, mg	264	396	528	595	661
Cr (VI) removal percentage If reaction period is 370 min, %	57.69	68.18	82.03	91.3	100
Kinetic Coefficient (k), mg/L.min	0.0544	0.0868	0.1148	0.1215	0.1308
Reaction time to complete photoreduction of Cr (VI), min	909	588	435	400	370

The information relative to the result of this part was presented in Table 4.9. The best condition providing highest efficient was found when the TiO_2 coating surface area was 0.2924 m^2. That was coated with 661 mg of TiO_2 which the maximum TiO_2 was coating surface area using in this work. The kinetic coefficient values of each condition were shown in Table 4.9 presented that TiO_2 coating surface area was also the important parameters controlling the efficiency of chromium (VI) removal because TiO_2 coating surface area was the direct function of amount of catalyst which provide photoactivity.

However, the increasing of TiO_2 coating surface area provided the increasing of reaction rate or kinetic coefficient value. However, the photoreaction was limited by the inputting energy which came from the ultraviolet lamps and the capacity of the light emitting to the discs plate, which related to the positions between the light source and the disc plates. These reasons as well agree with the result of previous worked by Dionysiou (2002) research.

4.8 Effect of initial concentration of synthesis wastewater in the operating of RDPR.

To study effect of initial concentration of synthesis wastewater on chromium (VI) removal efficiency, the experimental conditions used in all concentrations represented in Table 4.10. From the results of previous parts, they have shown that all studies parameters (initial pH of wastewater, flow rate of wastewater, rotation of disc and TiO_2 coating surface area) were affected to the chromium (VI) removal efficiency by using RDPR. In this part, initial concentration of wastewater was varied as of 25, 40, 50, 80, 100,150, 250, 300 and 500 ppm.

Table 4.10 Experimental details in the study of the effect of initial concentration of wastewater on chromium (VI) removal efficiency.

Function	amount
Wastewater flow rate (Q_w), mL/sec	90
Rotating disc speed (V_r), rpm	200
TiO_2 coating surface area, m^2	0.234
Height of wastewater in RDPR, cm	5
Initial pH of wastewater	3
Rate of N_2 Gas input, L/min	4.5

4.8.1 Effect of initial concentration of synthesis wastewater in the range of 25 – 100 ppm to the operating of RDPR.

The photoreduction of chromium (VI) in the varying initial concentration of synthesis wastewater in the range of 25 – 100 ppm were shown in Figure 4.18. The results could explain that the reactions needed longer time to complete the removal of

chromium (VI) in the high concentration. As the concentration of chromium (VI) 100 ppm, it needed 585 minute for complete removed. Otherwise, 25 ppm of synthesis wastewater used merely 105 minute for successfully treatment. The reaction rates of all concentrations were presented in Figure 4.19. The reaction rates of photoreduction in chromium (VI) rapidly decrease between 25 to 40 ppm. And it slowly decreased in the range of 50 to 100 ppm. Then, the results were shown that the kinetic coefficient constants (k) were decrease when increased the initial concentration of wastewater as shown below.

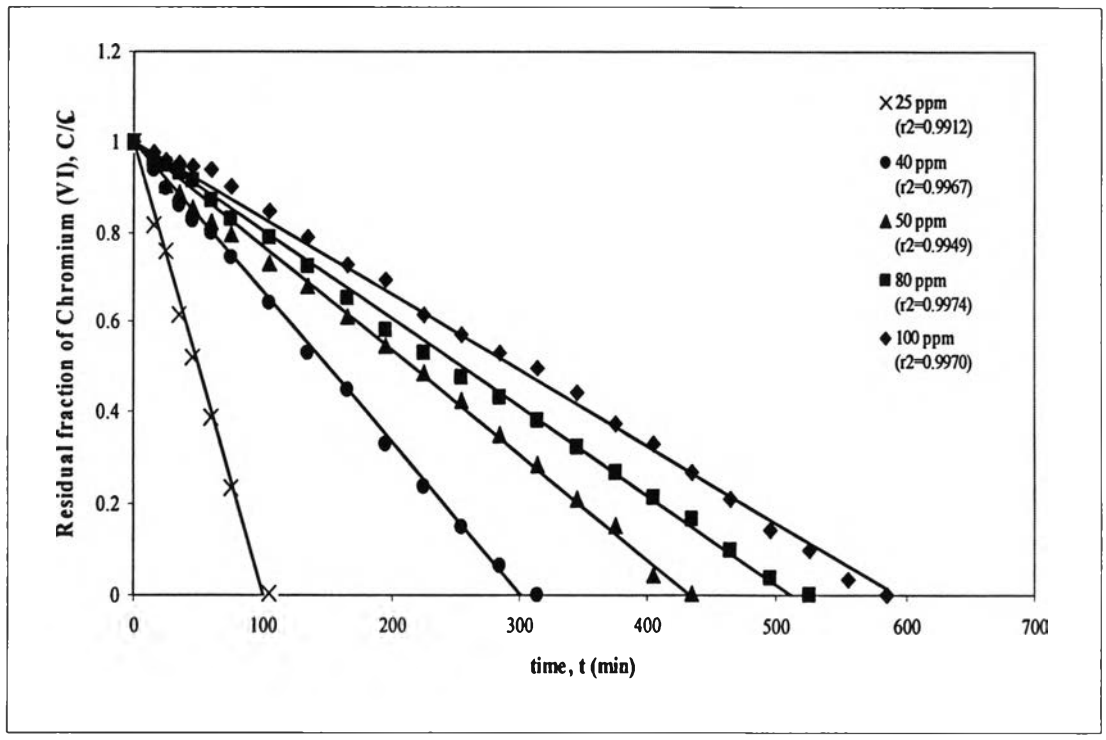

Figure 4.18 Residual fraction of chromium (VI) on time in different initial concentration of synthesis wastewater in the range of 25 - 100 ppm.

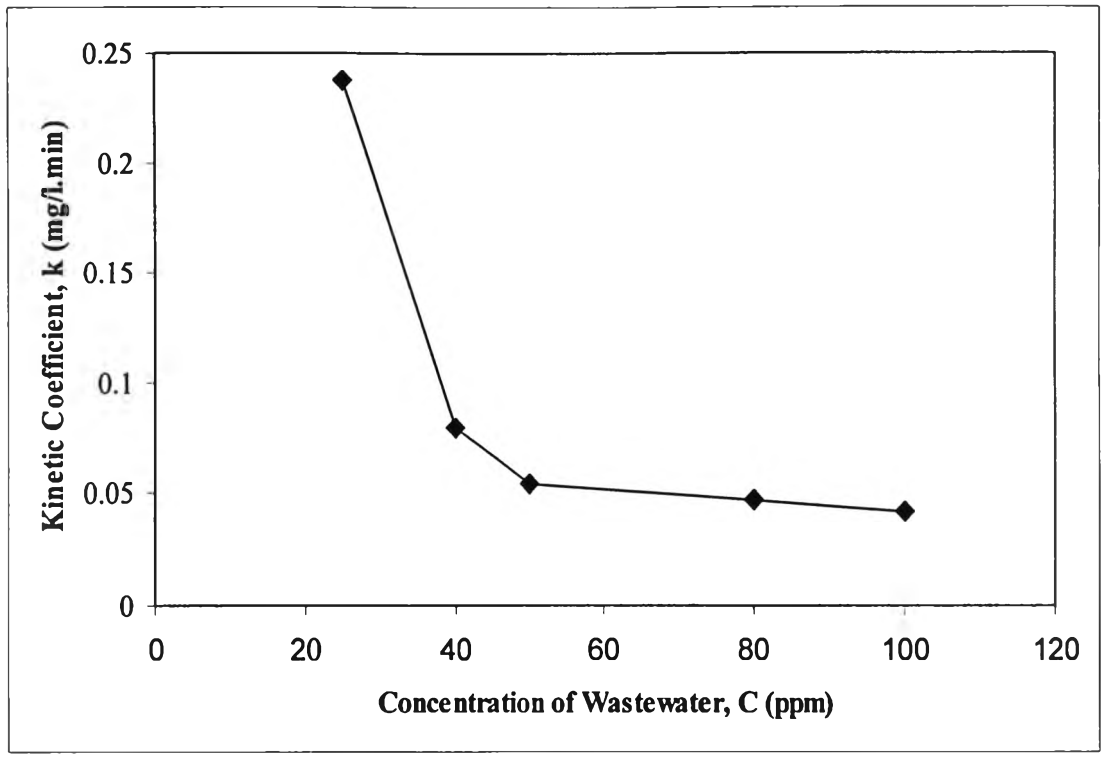

Figure 4.19 Kinetic coefficients (k) of residual chromium (VI) with different concentration of synthesis wastewater in the range of 25 to 100 ppm.

Table 4.11 Experimental conditions of each experiment in varying initial concentration of wastewater in the range of 25 – 100 ppm.

Experimental condition	Experiment No.				
	1	2	3	4	5
Initial concentration of wastewater, ppm	25	40	50	80	100
Cr (VI) removal percentage If reaction period is 105 min, %	100	33.33	24.14	20	17.95
Kinetic coefficient (k), mg/L.min	0.2375	0.08	0.055	0.0475	0.0425
Reaction time to complete photoreduction of Cr(VI), min	105	315	435	525	585

4.8.2 Effect of initial concentration of synthesis wastewater in the range of 150 – 500 ppm to the operating of RDPR.

The residual fraction of chromium (VI) in the varying initial concentration of synthesis wastewater in the range of 150 – 500 ppm was show in Figure 4.20.

To compare the photocatalytic activity of the initial concentration of wastewater, the efficiency and the kinetic coefficient (k) or reaction rate of chromium (VI) removal were determined by fitting the statistically with the experimental information. The photocatalytic reaction with respect to initial concentration of the solution can be explained as the kinetic coefficient (k) with the equation below.

$$d[C]/dt = -k_{obs}[C]^n \qquad (4.3)$$

Where k_{obs} is the kinetic coefficient or reaction rate

n is the order of the reaction

When $n = 0$, the reaction is *Zero-order*. *Zero-order* reaction is one in the rate of reaction independent of the concentration of solution. *Zero-order* equation present in equation (2).

$$d[C]/dt = -k_{obs}[C]^0$$

$$C - C_o = -k_{obs}.t \qquad (4.4)$$

When $n = 1$, the reaction is *First-order*. *First-order* reaction is respect to the concentration (C) of the solution, *First-order* equation show below in equation (3).

$$d[C]/dt = -k_{obs}[C]^1$$

$$d[C]/[C] = -k_{obs}.dt$$

$$ln[C/C_o] = -k_{obs}.t \qquad (4.5)$$

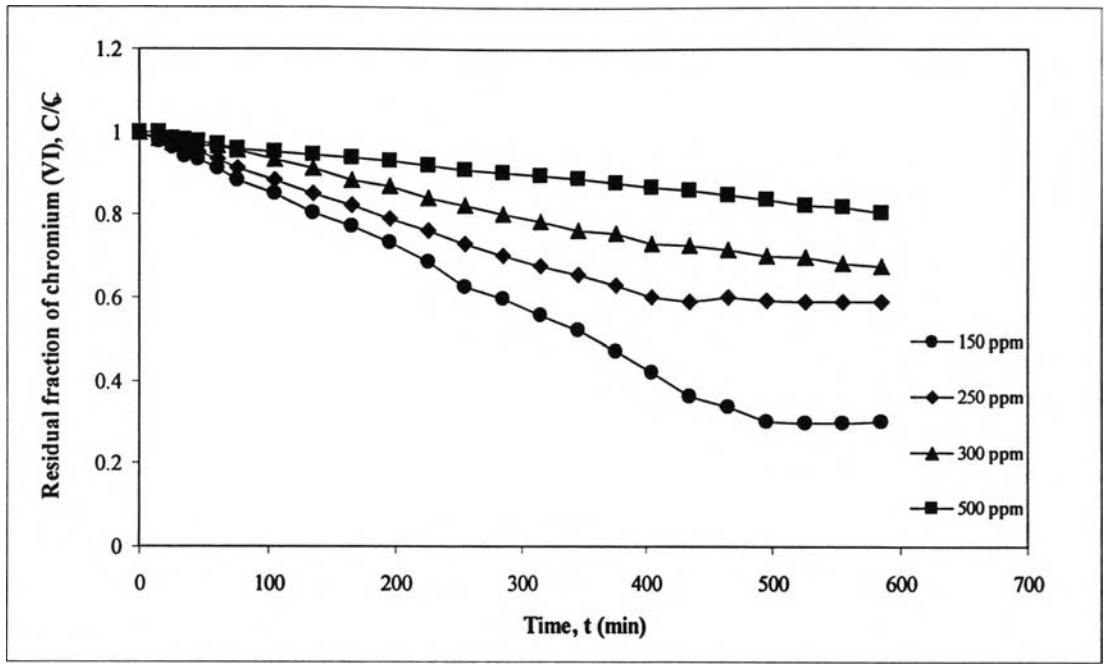

Figure 4.20 Residual fraction of chromium (VI) on time in different initial concentration of wastewater in the range of 150 - 500 ppm.

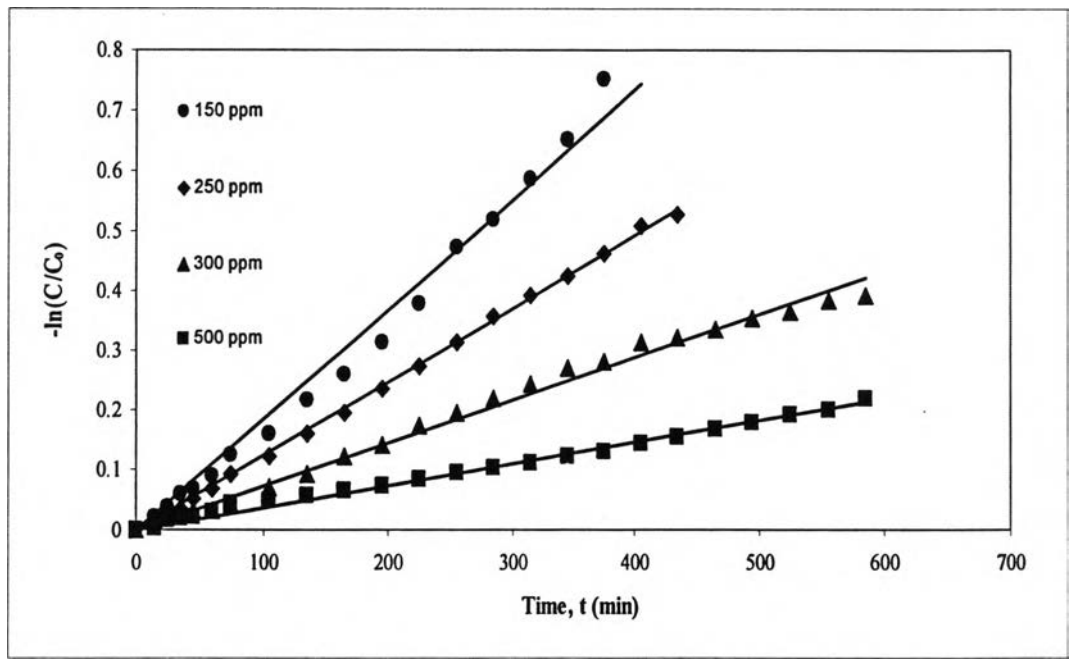

Figure 4.21 Show the relation between $-\ln(C/C_0)$ and time in different initial concentration of wastewater in the range of 150 - 500 ppm.

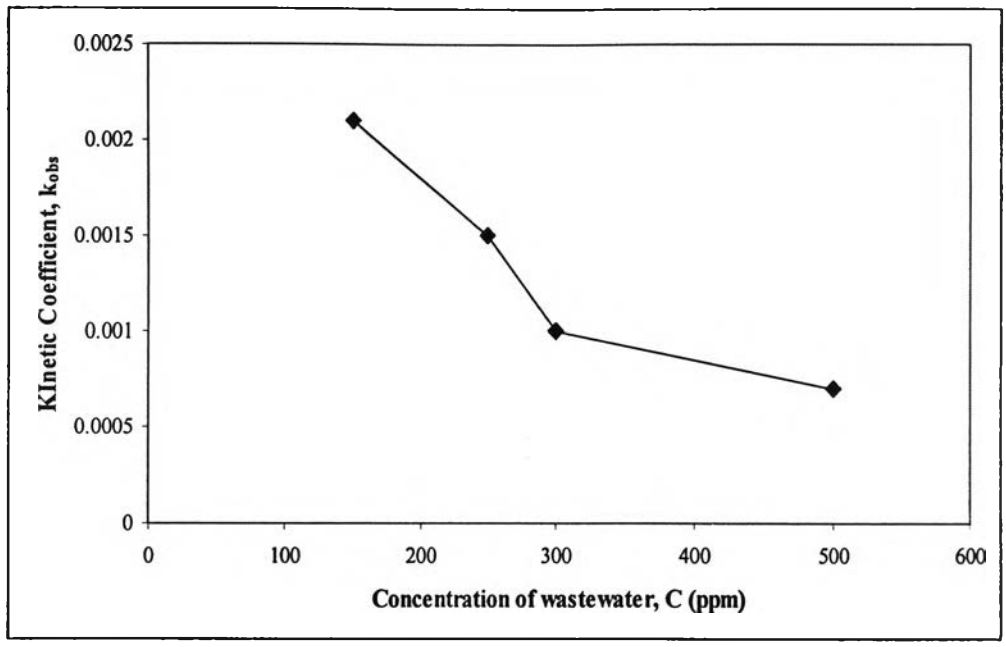

Figure 4.22 Kinetic coefficients (k_{obs}) of residual chromium (VI) with different concentration of synthesis wastewater in the range of 150 – 500 ppm.

Table 4.12 The comparison of reaction order in the different concentration of synthesis wastewater in the range of 150 – 500 ppm.

Concentration (ppm)	**Zero order**		**pseudo-first order**	
	kinetic coefficient (k), mg/L.min	r^2	kinetic coefficient (k_{obs}), min^{-1}	r^2
150	0.2136	0.9991	0.0021	0.9896
250	0.2581	0.9967	0.0015	0.9989
300	0.1456	0.9815	0.0010	0.9952
500	0.1679	0.9885	0.0007	0.9921

In this experimental part, the results exhibited that the maximum concentration of chromium (VI) which this reactor could completely removal was approximated 100 ppm, the result from Figure 4.18. In the condition of 90 mL/secec, rotation disc speed 200 rpm and initial pH of wastewater was 3 can completely remove 100 ppm of

chromium (VI) in about 10 hours as shown in Figure 4.18. Moreover, when increasing the initial concentration of wastewater it was reduced the efficiency in the removal rate which the same condition as shown in Figure 4.20. In kinetic consideration, the chromium (VI) removal was representing in zero order pattern with the capacity of this reactor less than and equal to 150 ppm. And the chromium (VI) removal was representing in pseudo-first order pattern with the capacity of this reactor more than 150 ppm as shown the consideration in Table 4.12.

The Langmuir Hinshewood rate expression has been successfully used for heterogeneous photocatalytic degradation to determine the relationship between the initial degradation rate and the initial concentration of chromium (VI) (Chen et al., 1998):

$$\frac{1}{k_{obs}} = \frac{1}{k.K_{Cr(VI)}} + \frac{[Cr(VI)]_0}{k} \qquad (4.6)$$

Where $[Cr\ (VI)]_0$ is the initial concentration of chromium (VI) in the unit of m/l,

$K_{Cr\ (VI)}$ is the Langmuir Hinshewood adsorption equilibrium constant in the unit of l/mg

k is the second order rate constant of surface reaction in the unit of mg/L.min

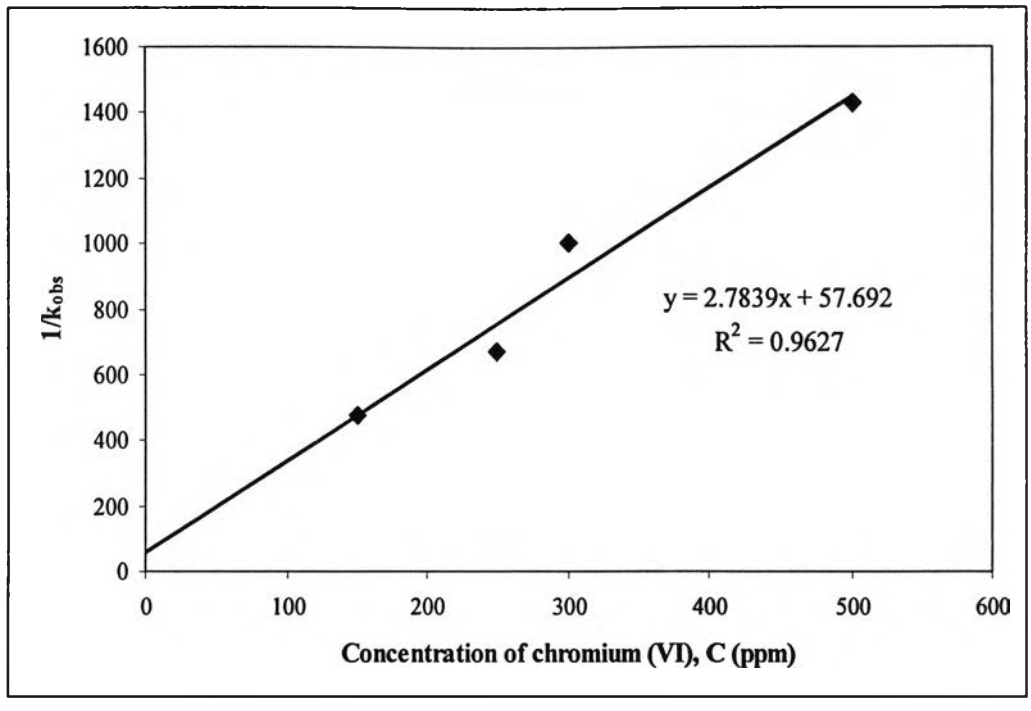

Figure 4.23 Determination of the adsorption equilibrium constants and degradation rate constants for chromium (VI).

From Figure 4.23, the second order rate constant of chromium (VI), k in the range of initial concentration of 150 to 500 ppm can determine 0.3592 mg/L.min and the adsorption equilibrium constant, $K_{Cr\,(VI)}$ was 0.0482 l/mg.